

## SUPPORTING INFORMATION

### **A bio-inspired heterodinuclear CoFe complex of the hydrogenases**

Lili Sun,<sup>a,\*</sup> Suzanne M. Adam,<sup>a,b,\*</sup> Walaa Mokdad,<sup>a</sup> Rolf David,<sup>a</sup> Anne Milet,<sup>a</sup> Vincent Artero,<sup>b,\*</sup> Carole Duboc<sup>a,\*</sup>

<sup>†</sup>Univ Grenoble Alpes, CNRS UMR 5250, DCM, F-38000 Grenoble, France

<sup>‡</sup>Univ Grenoble Alpes, CNRS, CEA, Laboratoire de Chimie et Biologie des Métaux, F-38000 Grenoble, France

\* equal contribution of the co-authors

**General.** All common reagents were purchased and used as received without further purification with the exception of the following: ferrocene was freshly sublimed before use, THF was distilled over Na/benzophenone, and all solvents were dried over molecular sieves and degassed with Ar before use in experiments. The ligand ( $L^{N_2S_2} = 2,2'-(2,2'-bipyridine-6,6'-diyl)-bis(1,1-diphenyl-ethanethiolate)$ ) and complexes,  $[Co^{II}(L^{N_2S_2})]$  and  $[Fe^{II}(MeCN)_2(CO)Cp]BF_4$ , were prepared according to previously published methods,<sup>11,14,16</sup> and preparation of all other coordination complexes was performed in a glove box under Ar atmosphere according to the procedures outlined below.

**Characterization methods.** X-band EPR solid state or frozen solution (5 mM in deaerated DMF) samples were prepared in the glove box in a quartz EPR tube. Spectra were acquired on a Bruker EMX instrument equipped with the ER-4192 ST Bruker cavity and an ER-4131 VT probe. Acquisition parameters: 15 dB, 100 K under flow of liquid nitrogen. IR measurements were recorded as the average of 4 scans for solid powder samples of the complexes in the glove box (Ar) on an Agilent Cary 630 FTIR spectrometer equipped with an attachment for diamond attenuated total reflectance measurements. Absorption spectra were recorded on a ZEISS MC5601 spectrophotometer in a quartz cell (path length: 1 mm). ESI-MS experiments were performed in positive ionization mode on a Bruker Esquire 3000 Plus ion trap spectrometer equipped with an electrospray ion source.

**Electrochemistry.** Cyclic voltammograms were recorded in a glove box (Ar) equipped with a Metrohm Autolab B.V. potentiostat. Unless otherwise noted, the following parameters and experimental conditions were used: electrolyte: 0.1 M  $(Bu)_4NClO_4$  in DMF; concentration of the complex: 1 mM; reference electrode: Ag/AgNO<sub>3</sub> in DMF/electrolyte; counter electrode: Pt wire; scan rate: 100 mV/s; working electrode: 3 mm diameter glassy carbon disk polished with 2mm diamond paste. All potentials were internally calibrated to the  $Fc^{+/0}$  couple using freshly sublimed ferrocene.

**DFT details.** All complexes were optimized to a minimum with the Gaussian09<sup>1</sup> program using the BP86<sup>2</sup> (and B3P86<sup>3</sup>) functional and a def2-TZVP<sup>4</sup> basis set. Frequencies calculations were performed to ensure that the complexes were optimized to their respective minima. Implicit solvation was performed using the IEFPCM scheme<sup>5</sup>.

To calculate theoretically the redox potential both the complex couple ( $[Co^{II}Fe^{II}]^+/[Co^IFe^{II}]$ ) and the reference complex couple ( $[Fc]^+/[Fc]$ ) were optimized in acetonitrile (as an implicit solvent i.e., the solvent is represented by a dielectric constant) as proposed by Konezy et al<sup>6</sup>.

The free energy difference between  $[\text{Co}^{\text{II}}\text{Fe}^{\text{II}}]^+$  and  $[\text{Co}^{\text{I}}\text{Fe}^{\text{II}}]$  was calculated as well as the free energy difference between  $[\text{Fc}]^+$  and  $[\text{Fc}]$ . Following that and using the following equation (equation 1), the absolute redox potentials of both the complex  $[\text{Co}^{\text{II}}\text{Fe}^{\text{II}}]^+$  and the reference complex (RC) was obtained.

$$E_{\text{abs}}([\text{Co}^{\text{II}}\text{Fe}^{\text{II}}]^+ / [\text{Co}^{\text{I}}\text{Fe}^{\text{II}}]) = \frac{-\Delta G}{nF} = \frac{-(G([\text{Co}^{\text{I}}\text{Fe}^{\text{II}}]) - G([\text{Co}^{\text{II}}\text{Fe}^{\text{II}}]^+))}{nF} \quad (1)$$

$$E_{\text{abs}}([\text{Fc}]^+ / [\text{Fc}]) = \frac{-\Delta G}{nF} = \frac{-(G([\text{Fc}]) - G([\text{Fc}]^+))}{nF} \quad (2)$$

The redox potential of complex  $[\text{Co}^{\text{II}}\text{Fe}^{\text{II}}]^+$  referenced to the ferrocene/ferrocenium couple is thus calculated using the following equation:

$$E_{\text{calc}}([\text{Co}^{\text{II}}\text{Fe}^{\text{II}}]^+ / [\text{Co}^{\text{I}}\text{Fe}^{\text{II}}]) = E_{\text{abs}}([\text{Co}^{\text{II}}\text{Fe}^{\text{II}}]^+ / [\text{Co}^{\text{I}}\text{Fe}^{\text{II}}]) - E_{\text{abs}}([\text{Fc}]^+ / [\text{Fc}]) \quad (3)$$

The results are represented in Table S1.

### Syntheses.

$[(\text{L}^{\text{N2S2}})\text{Co}^{\text{II}}\text{Fe}^{\text{II}}(\text{CO})(\text{Cp})]\text{BF}_4$  (**Co<sup>II</sup>Fe<sup>II</sup>**). Solid  $[\text{Co}^{\text{II}}(\text{L}^{\text{N2S2}})]^{14}$  (100 mg; 0.157 mmol) was added to a stirring solution of  $[\text{Fe}^{\text{II}}(\text{MeCN})_2\text{COCp}]\text{BF}_4^{15}$  (50 mg; 0.157 mmol) in 10 mL dry, degassed dichloromethane in a glove box. The reaction was allowed to proceed overnight and the dark black-brown solid product was filtered and washed with EtOH and dried under vacuum. UV-vis: 468 nm ( $\epsilon = 4500 \text{ M}^{-1}\text{cm}^{-1}$ ), 584 nm ( $\epsilon = 2800 \text{ M}^{-1}\text{cm}^{-1}$ ); IR:  $1856 \text{ cm}^{-1}$  (strong); EPR: solid state, rhombic:  $g_x = 1.98$ ,  $g_y = 2.09$ ,  $g_z = 2.24$ ; ESI-MS:  $M = [(\text{L}^{\text{N2S2}})\text{Co}^{\text{II}}\text{Fe}^{\text{II}}(\text{CO})(\text{Cp})]^+ m/z = 786.04$  (786.09);  $[M-\text{CO}]^+ m/z = 758.06$  (758.09).

$[(\text{L}^{\text{N2S2}})\text{Co}^{\text{I}}(\text{CO})\text{Fe}^{\text{II}}(\text{Cp})]$  (**Co<sup>I</sup>Fe<sup>II</sup>**). A slight excess of solid cobaltocene (23.8 mg; 0.126 mmol) was added to a stirring solution of **Co<sup>II</sup>Fe<sup>II</sup>** (100 mg; 0.115 mmol) in 10 mL dry, degassed acetonitrile in a glove box. The reaction was allowed to proceed for 2 hours during which time the dark brown-black solution turns to a purple suspension. The solid was allowed to settle and isolated, washed with more acetonitrile and dried under vacuum. UV-vis: 522 nm ( $\epsilon = 5600 \text{ M}^{-1}\text{cm}^{-1}$ ), 950 nm ( $\epsilon = 3100 \text{ M}^{-1}\text{cm}^{-1}$ ); IR:  $1734 \text{ cm}^{-1}$  (strong); EPR: silent; ESI-MS:  $M = [(\text{L}^{\text{N2S2}})\text{Co}^{\text{I}}\text{Fe}^{\text{II}}(\text{CO})(\text{Cp})] m/z = 786.0$  (786.10).

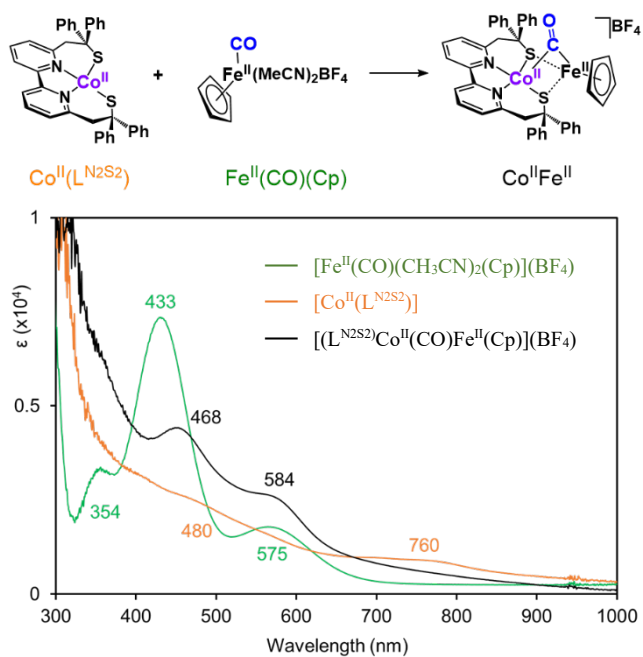


**Figure S1.** UV-visible spectra following the synthesis of  $\text{Co}^{\text{II}}\text{Fe}^{\text{II}}$  (black), from  $[\text{Co}^{\text{II}}(\text{L}^{\text{N}_2\text{S}_2})]$  (orange), and  $[\text{Fe}^{\text{II}}(\text{CO})(\text{CH}_3\text{CN})_2(\text{Cp})](\text{BF}_4)$  (green). Complex concentration = 0.1 mM in DMF.

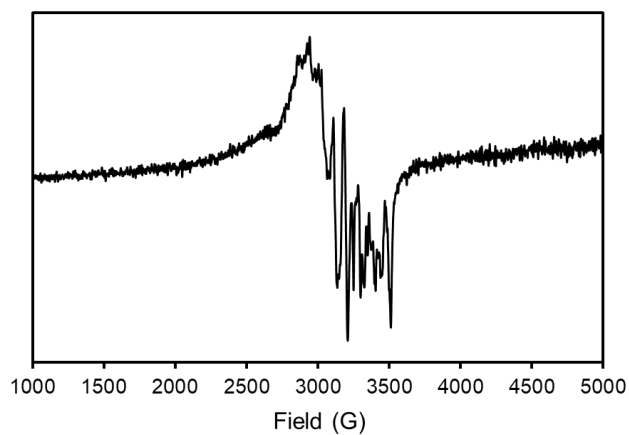


**Figure S2.** EPR spectra of the  $\text{Co}^{\text{II}}\text{Fe}^{\text{II}}$  complex in DMF glass (5 mM) at 100 K.

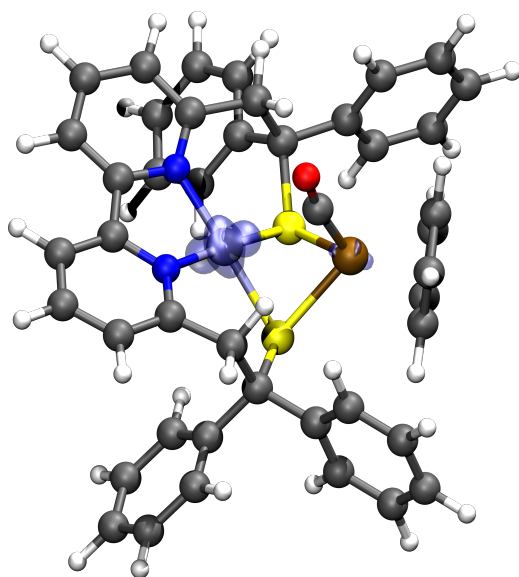


**Figure S3.** Representation of the (positive) spin density in light transparent blue for the  $\text{Co}^{\text{II}}\text{Fe}^{\text{III}}$  complex. Carbon, oxygen, nitrogen, hydrogen, sulphur, iron, and cobalt atoms are represented in grey, red, blue, white, yellow, ochre, and cyan respectively in a ball and stick manner.

**Table S1.** Energies of the quartet relative to the doublet for the  $[\text{Co}^{\text{II}}\text{Fe}^{\text{III}}]^+$  complex. Energies are expressed in kcal/mol.

	BP86	B3P86
Doublet	0	0
Quartet	21.71	13.18

**Table S2.** Calculated and experimental redox potential of the  $[\text{Co}^{\text{II}}\text{Fe}^{\text{III}}]^+ / [\text{Co}^{\text{I}}\text{Fe}^{\text{II}}]$  couple.

	Redox potential (V vs Fc)	
	BP86	B3P86
$E^{\circ}_{\text{calc}}$ (MeCN)	-0.56	-1.02
$E^{\circ}_{\text{exp}}$ (DMF)	-1.00	

**1** Frisch, M. J.; Trucks, G. W.; Schlegel, H. B.; Scuseria, G. E.; Robb, M. A.; Cheeseman, J. R.; Scalmani, G.; Barone, V.; Mennucci, B.; Petersson, G. A.; et al. Gaussian 09 Revision D.01. Gaussian Inc. Wallingford CT **2009**.

**2** (a) Becke, A. D. Density-Functional Exchange-Energy Approximation with Correct Asymptotic Behavior. *Phys. Rev. A* **1988**, *38*, 3098–3100. (b) Perdew, J. P. Density-Functional

Approximation for the Correlation Energy of the Inhomogeneous Electron Gas. *Phys. Rev. B* **1986**, 33, 8822–8824.

**3** (a) Becke, A. D. Density-Functional Thermochemistry. III. The Role of Exact Exchange. *J. Chem. Phys.* **1993**, 98, 5648. (b) Perdew, J. P. Density-Functional Approximation for the Correlation Energy of the Inhomogeneous Electron Gas. *Phys. Rev. B* **1986**, 33, 8822–8824.

**4** (a) Weigend, F.; Ahlrichs, R. Balanced Basis Sets of Split Valence, Triple Zeta Valence and Quadruple Zeta Valence Quality for H to Rn: Design and Assessment of Accuracy. *Phys. Chem. Chem. Phys.* **2005**, 7, 3297. (b) Weigend, F. Accurate Coulomb-Fitting Basis Sets for H to Rn. *Phys. Chem. Chem. Phys.* **2006**, 8, 1057.

**5** Tomasi, J.; Mennucci, B.; Cancès, E. The IEF Version of the PCM Solvation Method: An Overview of a New Method Addressed to Study Molecular Solutes at the QM Ab Initio Level. *J. Mol. Struct. THEOCHEM* **1999**, 464, 211–226.

**6** Konezny, S. J.; Doherty, M. D.; Luca, O. R.; Crabtree, R. H.; Soloveichik, G. L.; Batista, V. S. Reduction of Systematic Uncertainty in DFT Redox Potentials of Transition-Metal Complexes. *J. Phys. Chem. C* **2012**, 116, 6349–6356.